Asian Journal of Applied Chemistry Research

9(1): 1-15, 2021; Article no.AJACR.70878
ISSN: 2582-0273

Green Synthesis of Silver Nanoparticles using *Delonix regia* Extract, Characterization and its Application as Adsorbent for Removal of Cu (II) Ions from Aqueous Solution

Ahmed M. Abu-Dief[1,2*], Laila H. Abdel-Rahman[1], M. A. Abd– ElSayed[3] and Mallak Megalea Zikry[3]

[1]Chemistry Department, Faculty of Science, Sohag University, 82534 Sohag, Egypt.
[2]Department of Chemistry, College of Science, Taibah University, Madinah, P. O. Box-344, Saudi Arabia.
[3]Medicinal and Aromatic Plants Researches Department, Horti. Res. Institute (H.R.I.), Agri. Res. Center (A.R.C.), Giza, Egypt.

Authors' contributions

This work was carried out in collaboration among all authors. All authors read and approved the final manuscript.

Article Information

DOI: 10.9734/AJACR/2021/v9i130202
Editor(s):
(1) Dr. Angélica Machi Lazarin, State University of Maringá, Brazil.
Reviewers:
(1) Darwin F. Reyes, Nueva Ecija University of Science and Technology, Philippines.
(2) Rachadaporn Benchawattananon, Khon Kaen University, Thailand.
Complete Peer review History: https://www.sdiarticle4.com/review-history/70878

Original Research Article

Received 02 May 2021
Accepted 09 July 2021
Published 15 July 2021

ABSTRACT

In this research synthesis of silver nanoparticles by a green method is studied. The high importance of silver nanoparticles using extract of *Delonix regia* (DREAgNs) is due to their unique properties, such as non-expensive, easily available and have application in water treatment. Synthesized silver nanoparticles AgNPs were characterized using UV-Visible Spectrophotometer to indicate the synthesis of AgNPs by green methods. The maximum absorbance of UV-Vis. analysis at wavelength 464 nm. (FT-IR) spectra to indicate the functional groups of phytochemical compounds at *Delonix regia* extract (DRE) and the silver nanoparticles (DREAgNPs) and also shows the role of active chemical constituents in stabilization and reduction of (DREAgNPs). Based on the transmission electron microscopy image analyses (TEM) confirmed the formation of

**Corresponding author: Email: ahmed_benzoic@yahoo.com, amamohammed@taibahu.edu.sa;*

spherical DREAgNPs with a particle size range of 20-50 nm with an average particle size of 35 nm. The Cu^{2+} ion adsorption process was studied by (DREAgNPs). The Cu^{2+} ions removal efficiency (R. E.) is 88.4 % at an initial concentration 15 ppm. Removal efficiency (R. E.) decreases as the Cu^{2+} ion concentration increases. Furthermore, thermodynamic studies confirmed that the biosorption process was endothermic and the positive value of ΔG° is quite common when an ion-exchange mechanism applies in the biosorption. The Positive value of ΔS◦ suggested an increase in randomness during the biosorption. The Freundlich isotherm has a good fit with the experimental data (R_2 =0.99) compared to Langmuir isotherm (R_2 = 0.90). This study shows that DREAgNPs are available, low cost, effective and environment friendlly biosorbent for the removal of Cu^{2+} ions from aqueous environment.

Keywords: Eco friendly; silver nanoparticles (AgNPs); removal efficiency; Cu2+ ions; aqueous solution.

1. INTRODUCTION

Nanomaterials have great importance because of their properties compared to the same element with a bulk form. Nanomaterial show many properties such as optical, catalytic that depend on nanoparticles shape and size [1]. Methods used to synthesis nanoparticle by chemical techniques are hazardous and high expensive. Silver nanoparticles (AgNPs) synthesized by chemical, biological and green techniques have been studied [2,3]. Green methods for nanoparticles synthesis increase catalytic activity due to the high surface area [4]. Different plants extract have been studied for nanomaterials syntheses such as copper and zinc [5], gold and magnesium [6] and silver [7,8]. Silver has many applications and shows low toxic effect in human [9]. Silver nanoparticles exhibit a good effect on infection treatment, the antimicrobial mechanism of silver nanoparticles that damage the cell leading to the death of cell [10]. Silver nanoparticles have a great role in medicine which has anti- inflammatory and cytotoxic effects against tumor cells [11,12]. AgNPs produced from green methods exhibit a low toxicological effect against normal cells [13]. *Aloe vera [*14], *Cinnamon zeylanicum* [15], *Carica papaya [*16], *Desmodium triflorum* [17], *Ocimum sanctum* [18] can be used to synthesis of silver nanoparticles (AgNPs), we have chosen Flamboyant (*Delonix regia*) extract for the synthesis of silver nanoparticle (AgNPs) as reducing and capping agent. It is available in Shandawil Research Station. The present study focuses on the synthesis of silver nanoparticles, characterization and its application as an adsorbent to remove toxic heavy metal such as Cu^{2+} ions present in water. Heavy metals have a toxic effect that releases into the water and contaminates food and have a harmful effect on animals and human health. Methods can be used for the removal of toxic heavy metals from water, but these methods were non-effective and high cost. Many researchers studied agricultural materials such as *Moringa oliefera and Delonix regia* for removing heavy metals ions from aqueous solution [19-21].

2. EXPERIMENTAL METHODS

2.1 Material

Silver nitrate ($AgNO_3$) and copper chloride ($CuCl_2.\ 2H_2O$) were purchased from Sigma-Aldrich with a Purity ≥ 99.8 % and 99.999 % respectively Based On Trace Metals Analysis.

2.1.1 Plant collection

The *Delonix regia* were collected from Sohag, Egypt (Shandawil Research center). This plant was chosen for this study due to its major role in reducing silver ions.

2.1.2 *Delonix regia* extract preparation

The fresh pods collected were cleaned with double distilled water. The pods were cut into small parts and 25 g was weighed out and added to 250 mL distilled water and heated at 60° C, filtered using filter paper and then stored at 4° C as *Delonix regia* extract (DRE) for further use.

2.1.3 Preparation of aqueous solution

We prepared a Stock solution of Ag^+ ions by weighing out 0.17 g of $AgNO_3$ and dissolved in a 200 ml flask, the result concentration was 5 mM.

We prepared a Stock solution of Cu^{2+} ions by weighing out 2.68 g of ($CuCl_2.\ 2H_2O$) and dissolved in a 1000 ml volumetric flask, the result concentration was 1000 ppm.

2.1.4 Synthesis of DREAgNPs

A 10 mL DRE was added to a 190 mL (2 mM silver nitrate ($AgNO_3$)) under stirring. The color of the mixture changed from pale yellow to dark-brown within 10 minutes, this indicated the formation of (DREAgNPs**).** By centrifuging the solution a precipitate of (DREAgNPs**)** was produced.

2.2 Characterization of DREAgNPs

The importance of characterization is to understand the shape and size of DREAgNPs. It gives information about DREAgNPs. We carried out the characterization using UV–vis. spectroscopy, Fourier Transform-Infrared Spectroscopy (FT-IR) and the Transmission Electron Microscopy (TEM) for DREAgNPs.

2.3 Instruments

A UV– Vis. spectrophotometer (Shimadzu UV-PC, Mumbai, India) with a resolution of 1nm between 200 and 800nm was used to indicate the formation of AgNPs. (FT-IR) spectroscope (FTIR-2000, Perkin-Elmer) to indicate the functional groups of phyto chemical compounds at plant extract which capped the silver nanoparticles (DREAgNPs) in the range of 200 – 4000 cm^{-1} wavelength. The morphology and particle size of the AgNPs was characterized by the Transmission Electron Microscopy (TEM, Philips model CM 200, Tokyo, Japan), the analysis samples were prepared and dropped onto the carbon coated-copper grid, after drying the copper-coated grid subjected TEM analysis. The dark-brown liquid was centrifuged (E- B- A, 20 zentrifugen78532 Tuttlingen) for 35 minute to obtain the silver nanoparticles, (Atomic Absorption Spectroscopy) (Perkin Elmer - Analyst, 200) were used to determine the concentration of Cu^{2+} ions.

2.4 Batch Biosorption Experiments

2. 4.1 Effect of initial metal ions concentration on biosorption of Cu^{2+} ions

50 ml (15, 20, 35, 40 ppm) of Cu^{2+} ions solution was added to 300 mg of silver nanoparticles (DREAgNPs) in a bottle at room temperature (25 °C) and the mixture was stirred for 1 hr.

2. 4.2 Effect of particle size of AgNPs on biosorption of Cu^{2+} ions

Biosorption experiments were carried out at different particle sizes of AgNPs (20 , 50, 100, 500 nm), 50 ml of Cu^{2+} ions solution of initial concentration (15 mg/L) was added to 300 mg of the biosorbent in 250 ml flat bottom bottle at room temperature (25 °C) and a different particle size of AgNPs. Then the mixture was stirred for 1 hour.

2.4.3 Effect of biosorbent dosage of AgNPs on biosorption of Cu^{2+} ions

In each biosorption experiment, 50 ml of Cu^{2+} ions solution of initial concentration (15 mg/L) was added to different dosages of the biosorbent (25, 50, 100, 200, and 300 mg) in 250 ml flat bottom bottle at room temperature (25°C) and the mixture was stirred for 1 hr.

2. 4.4 Effect of contact time on biosorption of Cu^{2+} ions

In the biosorption experiment, 200 ml of Cu^{2+} ions solution of different initial concentrations (15, 30 and 50 mg/L) was added to 1.2 g of the biosorbent in a 250 ml flat bottom bottle at room temperature (25°C) and the mixture was stirred on a shaker at 300 rpm with a contact times (10, 30, 50, 70 and 90) minutes**.**

2.4.5 Effect of temperature on biosorption of Cu^{2+} ions

Experiments on the effects of temperature on the biosorption of Cu^{2+} ions were done at different temperature (25° C, 30° C, 40° C and 60° C). 50 ml of different concentrations (15 , 30 and 50 mg/L) of Cu^{2+} ions solution was added to 300 mg of the biosorbent in 250 ml flat bottom bottle at different temperatures and the mixture was stirred for 1 hr.

After each experiment, the mixture was centrifuged. The concentration of the supernatant (Cu^{2+} ions) was determined using Flame Atomic Absorption Spectrometer.

The overall experiment was repeated three times for precision.

2.4.6 Calculation of Cu^{2+} ions absorption

The removal efficiency of the Cu^{2+} ions was determined using;

$$R.E.\ \% = \frac{(C_o - C_e)}{C_o} x\ \ 100 \qquad (3)$$

Where, R. E. % is the percentage of the removed Cu^{2+} ions.

3. RESULTS AND DISCUSSION

3.1 Characterization of the Prepared AgNPs

3.1.1 UV-visible spectral analysis

Characterization of *Delonix regia* extract (DRE) and silver nanoparticles (DREAgNPs) was first carried out using a UV-Visible absorption spectrometer (Fig. 1). Adding Delonix regia extract to ($AgNO_3$) solution, the mixture becomes a dark–brown color. The chemical compound in the *Delonix regia* extract (DRE) plays as a reducing and capping agents help reduction of Ag^+ ion and forming silver nanoparticles (DREAgNPs) [22]. Color change because of surface plasmon Resonance (S.P.R.) of silver nanoparticles (DREAgNPs). The absorption spectrum of DRE extract has a peaks observed due to chemical compound in the extract. A peak at 382 nm, which is typical for absorption of flavonoids and phenols and the peak at 292 nm in the spectra indicated the amino acid that have a role for reduction and stabilization of nanoparticles (DREAgNPs) [23,24,25]. The synthesized silver nanoparticles (DREAgNPs) show Surface Plasmon Resonance (SPR.) peak at 464 nm which suggests silver nanoparticles formation [26].

3.1.2 FT-IR analysis

We carried out FT-IR analysis of Delonix regia extract (DRE), silver nanoparticles Delonix regia (DREAgNPs) and (DREAgNP-Cu) (Fig. 2). Functional groups of (DRE) were indicated by FT- IR spectra. Region of 1000–1200 cm^{-1} has a peak that is characteristic of cellulose [27]. A peak at 3301 cm^{-1} due to O-H and N-H_2 groups that is indicating the presence of flavanols. The shift in the position of the peak to 3286 and 3279 cm^{-1} in the spectrum of the (DREAgNPs) and (DREAgNP-Cu) indicates the binding of Ag^+ and Cu^{2+} ions respectively with amino and hydroxyl groups [28]. The band at 1076 cm^{-1} is due to the C-N stretch and the shift to 1073 and 1082 cm^{-1} because of binding Ag^+ and Cu^{2+} ions with the C-N group respectively [29]. Peak was observed at 1638 cm^{-1}, may be due to the amide bond of proteins arise from the carbonyl stretching, and is shifted to wavenumber of 1635 and 1633 cm^{-1} indicates the binding of Ag^+ and Cu^{2+} ions respectively with carbonyl groups [30]. The spectrum at 1394 is due to the stretching of –C–O and –C–O–C. and shifted to 1387 and 1372 cm^{-1} after Ag^+ and Cu^{2+} ions binding respectively, this confirms the bonding between Ag^+ , Cu^{2+} ions and –OH/COO– groups at protein [31–33]. The synthsized silver nanoparticles show many peaks present in the DRE this due to the phyto chemical compound in the *Delonix regia* extract as capping and reducing agent of Ag^+ to Ag^0 and forming AgNPs [34,35] and help in biosorption of Cu^{2+} ions.

3.1.3 TEM analysis the synthesized AgNPs

The TEM technique was performed to visualize the synthesized AgNPs particle size and to study morphology. From the TEM image (Fig. 3), it is evident that most of the AgNPs were spherical. Characterization of accurate structural size and morphology analysis of AgNPs was examined using TEM. The TEM images of AgNPs were spherical in shape. The average diameter of the nanoparticlesvaries between 20 and 50 nm.

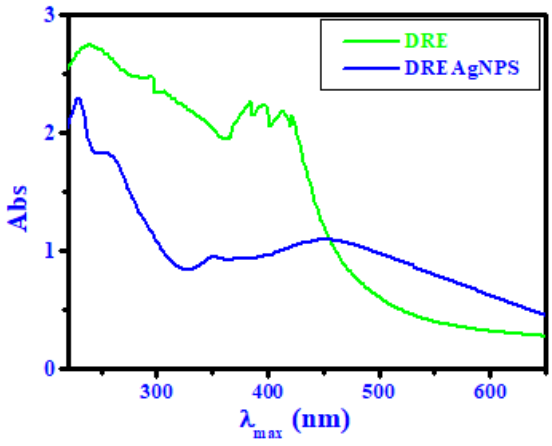

Fig. 1. UV–vis. spectra of DRE and DREAgNPs

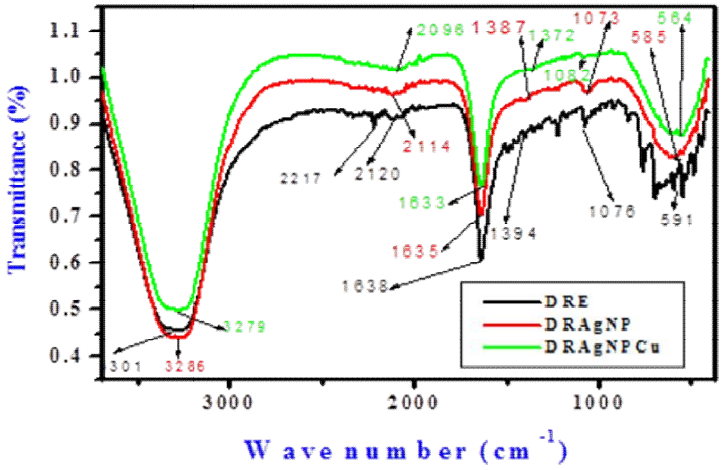

Fig. 2. FT-IR spectra of DRE, Ag^{+} loaded *Delonix regia* extract (DREAgNPs) and (DREAgNP-Cu)

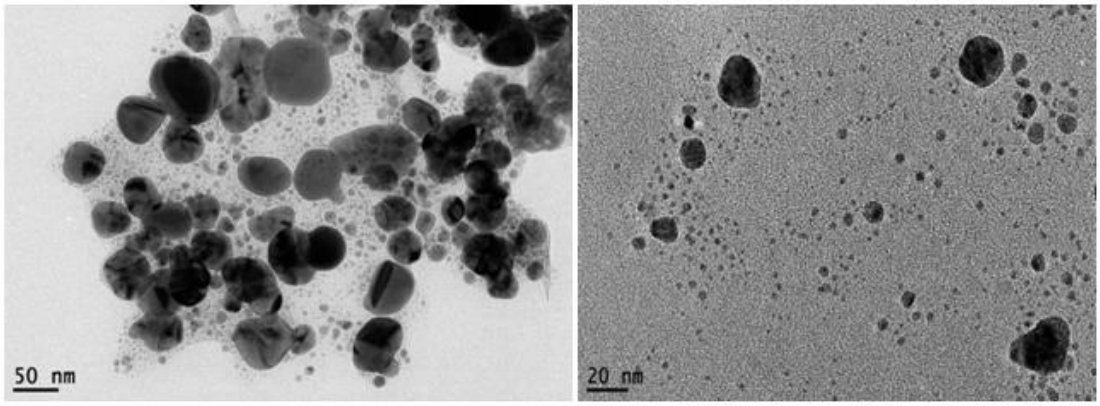

Fig. 3. Size and surface morphology of synthesized DREAgNPs by TEM

3.2 Adsorption of Cu^{2+} Ions by the Prepared AgNPs

Adsorption of heavy metals ions from an aqueous solution on the surface of adsorbents is a rather complex process affected by several factors. The effect of experimental parameters such as dose, particle size, initial concentration, contact time and temperature on the biosorption was studied. The adsorption mechanisms of heavy metals onto the adsorbent vary widely and depend upon the heavy metals under investigation and the type of adsorbent. Most adsorbents interact with metallic species through binding of the metal ion and the active sites on the surface of the adsorbent.

The synthesized silver nanoparticles (DREAgNPs) is a good adsorbent for adsorption the Cu^{2+} ions from the aqueous solution because of a high surface area as well as a phytochemical compound on the surface of synthesized silver nanoparticles (DREAgNPs) that play a major role in the bio-sorption of Cu^{2+} ions.

3.2.1 Effect of Cu^{2+} ions concentration on the bio-sorption of Cu^{2+} ion

Table 1 and Fig. 4 illustrated the effect of Cu^{2+} ions concentration on adsorption process by adsorbent (DREAgNPs). The Cu^{2+} ions removal efficiency (R. E.) for concentration 15 ppm are 88.4 and decreases as the concentration increases, this is due to a high chance was available of active site with functional group on the surface of adsorbent for metal ion removal at low concentrations. When increase the concentration of Cu^{2+} ions the removal efficiency

decreases this is due to active sites took up the available Cu^{2+} ions and a low chance was available of active site [36, 37].

This results close to the removal efficacy of Cr (III) and Cd (II) [37]. The highest removal efficiency was found for cadmium, i.e., 83.49 %, by using silver and NFC together as a bio sorbent. The cellulose acted as an adsorbent, where it makes an interface with the silver nanoparticles and enhances the efficacy. The second highest was for cadmium, i.e., 47.21 %, but by using only nano-fibrillated cellulose as a bio sorbent. The maximum sorption for both cadmium and chromium was observed with silver along with NFC, i.e., 83.49 % and 32.20%, respectively. In one set with cadmium containing silver as a biosorbent, after 40 min the metal-ion estimation which reduced showed an increase of 10 mg/lit at 80 min. This was because the adsorbate and adsorbent attained equilibrium and were incapable of further sorption [20,21, 37].

3.2.2 Effect of adsorbent dosage of AgNPs on the biosorption of Cu^{2+} ion

It is an important parameter to determine the capacity of the adsorbent for a given initial concentration 15 mg/L. The results obtained on the effect of adsorbent dosage on removal efficiency of Cu^{2+} ion biosorption by AgNPs was shown in Fig. 5 and Table 2.

As the increase in adsorbent dosage the metal ions, removal efficiency increases. Cu2+ ions removal efficiency was the lowest value (74.4 %) obtained with 25 mg and the highest value (88.4 %) with 300 mg of AgNPs adsorbent. This behavior is due to the increase in surface area and availability of biosorption sites. It was observed that the percentage removals of metal ions increased as the dosage of biosorbnt increased. This may be attributed to the increased adsorbent surface area, pores, active sites and the number of unsaturated sites of AgNPs adsorbent. [20,21].

Table 1. Cu^{2+} ions removal efficiency by AgNPs

Co (mg/L)	Ce(mg/L) ± SD	Cu^{2+} ions R. E. % ± SD
15	1.74±0.15	88.4±0.11
20	3.4±0.09	83±0.09
35	6±0.06	82.8±0.14
40	7±0.13	82.5±0.16

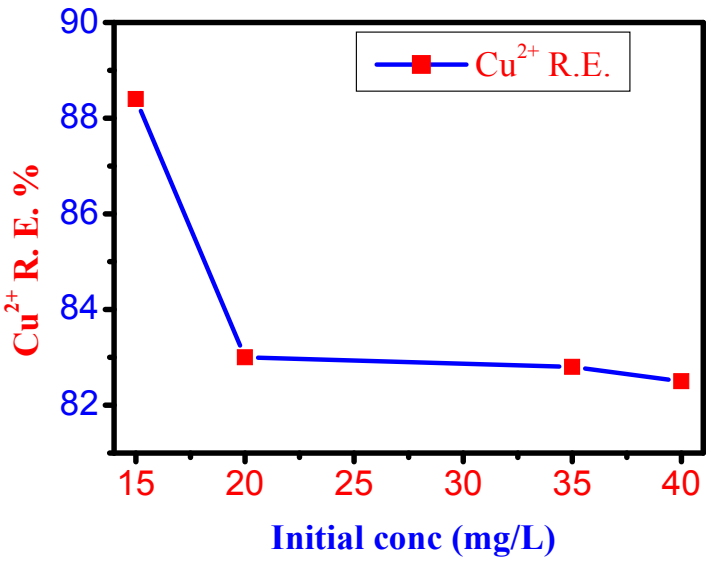

Fig. 4. Effect of Cu^{2+} ions concentration on removal efficiency by AgNPs

Table 2. Cu2+ ions removal efficiency at initial concentration of Cu2+ (15 mg/L) and different adsorbent dosage of AgNPs

Adsorbent dosage AgNPs (mg)	Ce(mg/L) ± SD	Cu^{2+} ions R. E. % ± Sd
25	3.84±0.06	74.4±0.07
50	3.62±0.07	75.86±0.23
100	2.98±0.09	80.13±0.20
200	2.84±0.08	81.06±0.26
300	1.74±0.06	88.4±0.18

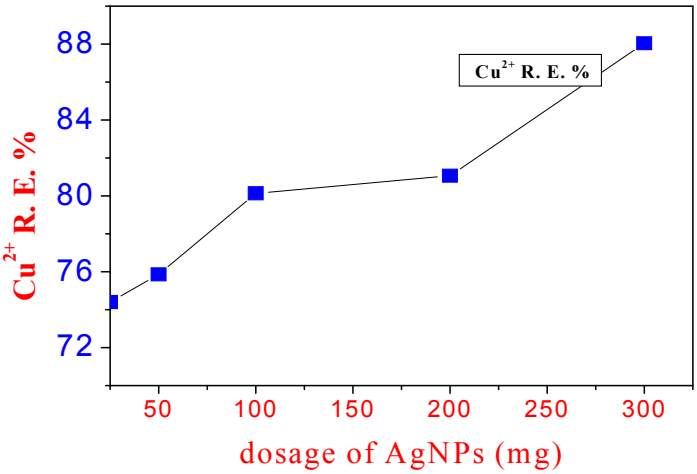

Fig. 5. Effect of adsorbent dosage of AgNPs on Cu^{2+} ions removal efficiency at initial concentration of Cu^{2+} (15 mg/L)

3.2.3 Effect of adsorbent particles size of AgNPs on the biosorption of Cu^{2+} ion

The effect of the adsorbent particle size was studied using different sizes of adsorbent as shown in Fig. 6, Table 3. It was noted that the removal efficiency % was very low when a larger particle size were used and this was probably due to the smaller surface area of the adsorbent. The R. E. % was very low 67.66 % when a larger particle size (500 nm) was used, and this was probably due to smaller surface area of the adsorbent. It was observed that the R.E. % was higher 88.4 % when the smaller particle nano size (20 nm) were used. It was observed that the removal efficiency % was higher when smaller particle nano sized were used, and this was probably due to higher surface area of the smaller nano-sized adsorbent. The decrease in adsorbents particle size increases the metal uptake. It is apparent that the greater surface area is increased by decreasing the adsorbents particle size. The number of active sites is increased as a result of the high particle surface area and therefore the ability of adsorbents structures is very high and the number of sorption sites for sorbent-solute interaction is increased, thereby resulting in increasing removal efficiency % from the solutions [20, 21].

3.2.4Effect of contact time on the biosorption of Cu^{2+} ion by adsorbent AgNPs

The results obtained from the effect of contact time on biosorption of Cu^{2+} ion by AgNPs was shown in Fig. 7 and Table 4 at initial metal ions concentrations of (15, 30 and 50 mg/L). It was observed that the amount of metal ion absorbed increased with an increase in contact time up to 70 minutes. This may be attributed to the long time of contact and availability of active sites, after the equilibrium is reached at 70 minutes, it was followed by a reduction in the metal uptake. The removal of metal ions was rapid at the initial period of the contact time and decreased slightly until the equilibrium is reached. The active sites

for biosorption are more available at the initial contact time and thus makes biosorption rate to be fast as a result of the diffusion process from the bulk solution to the sites. At longer contact time, there was a slightly increasing or remain constant in the metal ions removal, as the sites are less available as the capacity of the adsorbent gets exhausted, the rate of uptake was controlled by the rate at which the Cu^{2+} ion was transported from the solution to the sites of the adsorbent particles (AgNPs) [20, 21].

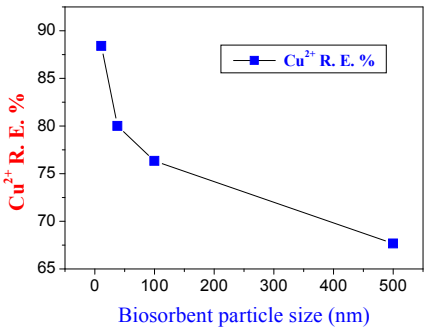

Fig. 6. Effect of adsorbent particle size of AgNPs on Cu^{2+} ions removal efficiency at initial concentration of Cu^{2+} (15 mg/L)

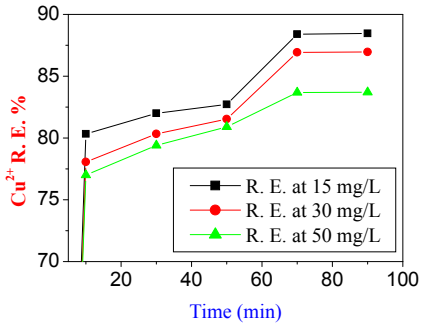

Fig. 7. Effect of contact time on Cu^{2+} ions removal efficiency at different initial concentrations (15, 30 and 50 mg/L) by the adsorbent (AgNPs)

3.2.5 Effect of temperature on the biosorption of Cu^{2+} ions by adsorbent AgNPs

The result obtained on the effect of the temperature at different values (25, 30, 40 and 60° C) on metal ions removal efficiency of Cu^{2+} ions biosorption by AgNPs was shown in Fig 8 and Table 5. It was noted that the Cu^{2+} ion removal efficiency at different initial concentrations (15, 30, 50 mg/L) by AgNPs increases while the temperature is increasing until a certain value that varies around 40 °C. The increase in adsorption capacity with temperature suggested that the active sites have increased with temperature. The increase of the temperature encourages the process of adsorption, until a certain temperature limit, around 40° C, which can be regarded as an optimal temperature. Beyond temperature limit around 40°C, at a higher temperature 60° C, the desorption becomes more important and reduces the rate of adsorption, this may be due to the breakdown of the phytochemical compound of the plant extract on the surface of the solid adsorbent AgNPs. This process due to increase in the movement of the metal ions which occurs at higher temperatures. The increase in adsorption with temperature may be due to increasment the interaction of the metal cation Cu^{2+} to the surface of adsorbent AgNPs leading to interaction occurring during adsorption process [20, 21].

3.2.5.1 Thermodynamic parameters of adsorption process

The thermodynamic parameters, ΔH, ΔS, and ΔG, for the biosorption process were calculated using the relationships (1) and (2) [38,39].

$$\ln b = \Delta S°/R - \Delta H°/RT \quad (1)$$

Where b (Langmuir constant related to energy). The plot of ln b versus 1/T yields a slope and intercept whose values correspond to ΔH/R and ΔS/R, respectively. These values can then be used to compute ΔG by applying the Gibbs relationship:

$$\Delta G° = \Delta H° - T\Delta S° \quad (2)$$

The Cu2+ions uptake at equilibrium was calculated using the relationships (3):

$$q_e = \frac{V(C_o - C_e)}{W} \quad (3)$$

where qe in mg/g is Cu 2+ ions absorption capacity, V in liters is the volume of the Cu2+ ions solution and W in gram is the amount of the biosorbent, Co and Ce in mg/L are initial and final (equilibrium) Cu2+ ion concentrations, respectively.

Adsorption isotherms of Cu^{2+} ions on DREAgNPs are presented as a function of the equilibrium concentration of metal ions in the aqueous

solution in Table 6 and Fig.9. The amount of Cu^{2+} adsorbed per unit mass of DREAgNPs increased with the initial concentration of Cu^{2+} as expected [40,41]. The metal ion distribution between the liquid and solid phases can be described by mathematical model equations such as the Langmuir isotherm model and the Freundlich isotherm model [42]. The Langmuir and Freundlich models are used because of their ability to describe experimental data in a wide range of concentrations. Freundlich and Langmuir's adsorption isotherms are also classical models to describe the equilibrium between metal ions adsorbed onto adsorbent and metal ions in solution. Both isotherm models can be easily transformed into linear forms, just by linear regression. Langmuir's isotherm model suggests that uptake take place on a homogeneous surface. These models could be summarized as follows. The linear form of the Langmuir isotherm equation is represented by the following equation(7) [43].

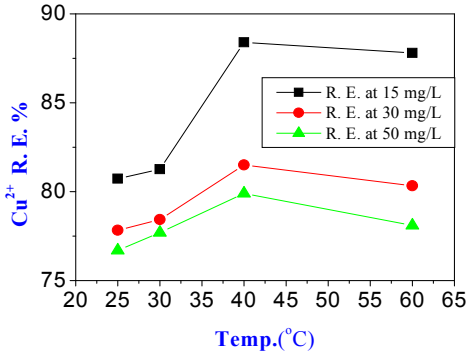

Fig. 8. Effect of temperature on Cu^{2+} ions removal efficiency at different initial concentrations (15, 30 and 50 mg/L) by the adsorbent (AgNPs)

$$C_e / q_e = 1/q_m b + C_e / q_m \quad (7)$$

as, q_e the amount of Cu^{2+} ions adsorbed at equilibrium (mg g^{-1} adsorbent), C_e is the equilibrium concentration of adsorbate (mg L^{-1}), b (L mg^{-1}) and q_m (mg g^{-1}) are the Langmuir constants related to energy and the adsorption capacity, respectively.

Plot of C_e/q_e against C_e give a straight line with slope $1/q_m$ and intercept $1/q_m$ b is obtained (Fig. 9), which shows Cu^{2+} biosorption isotherms of Langmuir. From the intercept and slope of the plots, the Langmuir parameters, b and q_m, are calculated. These values may be used for comparison and correlation of the sorptive properties of DREAgNPs.

The Freundlich equation is applicable for isothermal adsorption and has the general form (8). [44].

$$\log q_e = \log K_f + 1/n \log C_e \quad (8)$$

As, C_e is the equilibrium concentration (mg L^{-1}) of adsorbate, q_e is the amount of adsorbate (mg g^{-1} adsorbent). n and K_f are the Freundlich constants. When log q_e is plotted against log C_e, aline with slope 1/n and intercept log K_f is obtained (cf. Fig. 10). This reflects the satisfaction of the Freundlich isotherm model for the adsorption of Cu^{2+} ions. The intercept, log K_f, is an indicator of the adsorption capacity and the slope, 1/n, is an indicator of the intensity of adsorption [45]. The Freundlich parameters for the adsorption of Cu^{2+} ions is given in Table 7. To ascertain if the biosorption phenomenon is favorable or unfavorable, for Langmuir type biosorption process, isotherms can be classified by R_L, a dimensionless constant separator factor (9) [46] stated as:

$$R_L = 1 / (1 + b C_o) \quad (9)$$

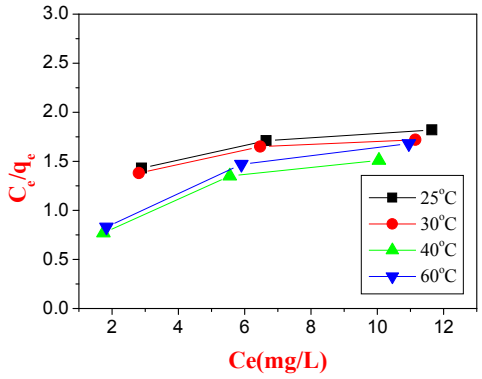

Fig. 9. Linearized biosorption isotherms of Langmuir

Mathematical calculation of R_L indicates the shape of isotherm to be either, irreversible (R_L = 0), linear (R_L = 1), unfavorable (R_L>1) or favorable (0 < R_L< 1). From the experiment, R_L varies from 0.139 to 0.676 for different Cu^{2+} ions concentrations (15, 30, 50) mg/L at different temperatures (cf. Table 9). These values ranged between 0 and 1, thus indicating a favorable

Table 3. Effect of the adsorbent particle size of AgNPs on the biosorption efficiency

Adsorbent particle size of AgNPs (nm)	Ce(mg/L) ± SD	Cu^{2+} ions R. E. % ± SD
20	1.74±0.06	88.4±0.18
50	3.0±0.11	80±0.13
100	3.55±0.08	76.33±0.22
500	4.85±0.14	67.66±0.15

Table 4. Effect of contact time on Cu2+ ions removal efficiency at different initial concentrations (15, 30 and 50 mg/L) by the adsorbent (AgNPs)

Temp. (o C)	Cu^{2+} R. E. % at Co (15)	Cu^{2+} R. E. % at Co (30)	Cu^{2+} R. E. % At Co (50)	C_e at Co (15)	C_e at Co (30)	C_e at C_o (50)
25	80.73	77.83	76.70	2.89	6.65	11.65
30	81.26	78.43	77.70	2.81	6.47	11.15
40	88.40	81.50	79.90	1.74	5.55	10.05
60	87.80	80.33	78.10	1.83	5.90	10.95

Table 5. Effect of temperature on Cu2+ ions removal efficiency at different initial concentrations (15, 30 and 50 mg/L) by the adsorbent (AgNPs)

Time (min)	Cu^{2+} R. E. % at C_o (15)	Cu^{2+} R. E. % at C_o (30)	Cu^{2+} R. E. % at C_o (50)	C_t at C_o (15)	C_t at C_o (30)	Ct at C_o (50)
10	80.33	78.06	77.00	2.95	6.58	11.50
30	82.00	80.33	79.40	2.70	5.90	10.30
50	82.72	81.53	80.90	2.59	5.54	9.55
70	88.40	86.93	83.68	1.74	3.92	8.16
90	88.46	86.96	83.70	1.73	3.91	8.15

Table 6. Values of the amount of Cu^{2+} ions adsorbed at equilibrium (q_e mg g^{-1} adsorbent) and the equilibrium concentration of adsorbate (C_e mg L^{-1}) for isotherms of Langmuir

Conc of $Cu2^{+}$ (mg/l)	C_e (mg/l)	q_e (mg/g) At 25 o C	C_e / q_e	C_e (mg/l)	q_e (mg/g) At 30 o C	C_e / q_e	C_e (mg/l)	Q_e mg/g At 40 o C	C_e / q_e	C_e mg/l	q_e mg/g At 60 o C	C_e / q_e
15	2.89	2.02	1.43	2.81	2.03	1.38	1.74	2.21	0.77	1.83	2.20	0.83
30	6.65	3.89	1.71	6.47	3.92	1.65	5.55	4.10	1.35	5.90	4.02	1.47
50	11.65	6.39	1.82	11.15	6.47	1.72	10.05	6.66	1.51	10.95	6.51	1.68

Table 7. values of the amount of Cu^{2+} ions adsorbed at equilibrium (qe mg g^{-1} adsorbent) and the equilibrium concentration of adsorbate (Ce mg L^{-1}) for isotherms of Freundlich

Conc of Cu^{2+}(mg/l)	Log C_e (mg/l)	Log q_e (mg/g)	Log C_e (mg/l)	Log q_e (mg/g)	Log C_e (mg/l)	Log q_e mg/g	Log C_e mg/l	Log q_e mg/g
15	0.47	0.31	0.49	0.31	0.25	0.34	0.26	0.34
30	0.82	0.59	0.82	0.60	0.74	0.61	0.78	0.6
50	1.07	0.81	1.05	0.81	1.002	0.82	1.04	0.81

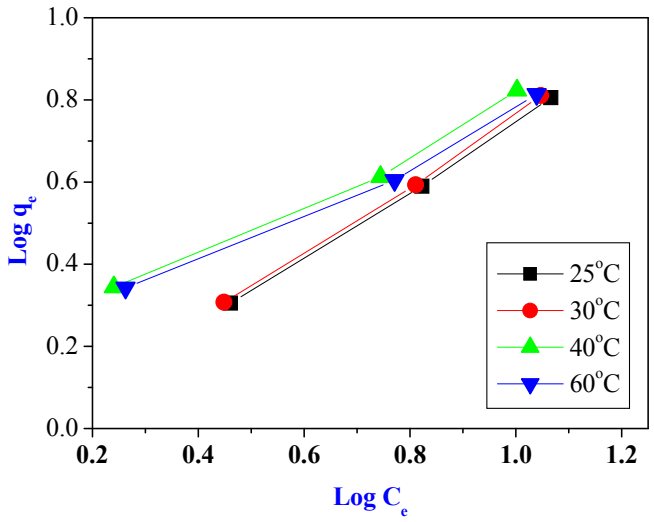

Fig. 10. Linearized biosorption isotherms of Freundlich

biosorption. The values of (Freundlich exponent n) were greater than1 [47]. Moreover, the value of n indicates better biosorption mechanism and formation of relatively stronger bond between adsorbate and biosorbent as 1/n values are found in the range of 0.595 – 0.833, when the temperature was altered from 293 to 323 K, this indicate that the biosorption of Cu^{2+} ions onto DREAgNPs is favorable under the conditions studied as 1/n values between 0 and 1. The fitting of the linear form of the models was examined by using linearity coefficient (R^2). The Langmuir model has a less fitting model than Freundlich model according to linearity coefficients (R^2 =0.90 and 0.99 respectively) as shown in Table 8 and Figs. 9 and 10. The sorption of Cu^{2+} ions onto DREAgNPs follow the Freundlich isotherm model describing the adsorption in aqueous system [39].

The obtained thermodynamics equilibrium constant was used to calculate all other thermodynamic parameters from a plot ln b against 1/T. The entropy, enthalpy and Gibbs free energy for the adsorption process were obtained at different temperatures for Cu^{2+} using Eq. (1). The sorption capacity of the DREAgNPs for Cu^{2+} increased with increasing temperature, this means the sorption process was endothermic. Thermodynamic parameters such as enthalpy change, free energy change and entropy change were determined using the equations (1), (2) [48]. Where ΔG° is the change in free energy (J mol^{-1}), ΔS° is the change in entropy (kJ mol^{-1} K^{-1}), ΔH° is the change in enthalpy (kJ mol^{-1}), R is the gas constants (8.314×10^{-3} kJ mol^{-1} K^{-1}), T is the absolute temperature (K), and b is the equilibrium constant of adsorption. When ln b is plotted against $1/T$, the slope $\Delta H°/R$, and intercept $\Delta S°/R$ are obtained. From the slope and intercept of the Van't Hoff plots of ln$b$ versus $1/T$ the values of ΔH° and ΔS° were obtained. The thermodynamic parameters are given in Table 10. Positive values of $\Delta H°$ suggest the endothermic nature of adsorption of Cu^{2+} ions on the DREAgNPs. The positive $\Delta G°$ values were obtained in this study. It has been suggested that a positive value for $\Delta G°$ is quite common when an ion-exchange mechanism applies in the biosorption of cationic sorbate because of the activated complex formed by the cationic sorbate (Cu^{2+} ions) with the biosorbent (DREAgNPs) [49]. The Positive value of ΔS° suggested an increase in randomness during the biosorption [50]. These kinds of reactions are present in literature [38,39,51].

3.2.5.2 Mechanism of adsorption

The capping agents of the phytochemical components of plant regulate nanoparticles and control the growth, agglomeration, and physico-chemical characteristics in a precise way [52]. The capping agent is an amphiphilic molecule comprising of a polar head group and a non-

Table 8. Isotherm constants of Cu^{2+} ions biosorption on DREAgNPs at various temperatures

T (K)	Langmuir			Friendlich		
	qm	b	R_2	n	K_f	R_2
298	23.1	0.032	0.90	1.22	0.86	0.999
303	25.3	0.030	0.85	1.20	0.846	0.998
313	11.43	0.124	0.87	1.62	1.53	0.987
333	10.96	0.121	0.88	1.68	1.50	0.987

Table 9. A dimensionless constant separator factor (RL) for Langmuir type biosorption process

Co(mg/L)	RL at 25°C	RL at 30°C	RL at 40°C	RL at 60°C
15	0.676	0.69	0.350	0.355
30	0.510	0.53	0.212	0.216
50	0.385	0.40	0.139	0.142

Table 10. Thermodynamic parameters for the biosorption process

Temperature (K)	ΔG° (KJ/mol)	ΔH°(KJ/mol)	ΔS° (KJ/mol)
298	8.36	34.7	0.0884
303	7.91		
313	7.03		
333	5.26		

polar hydrocarbon tail. Owing to the amphiphilic nature of capping agents, they confer the functionality and enhance the compatibility with another phase. The non-polar tail interacts with the encircling medium while the polar head interacts with the metal atom of the nanosystem [53]. The phytochemical compound-coated nanoparticles have adsorption ability to metal ions on the surface of it, and then the Cu-DREAgNPs complex can be separated by centrifugation, so used in the purification of drinking water. These silver nanomaterials are target-specific and do not produce any waste; therefore, it is a greener route for environmental remediation [54-56].

4. CONCLUSION

This study showed the synthesis of silver nanoparticles (DREAgNPs) using extract of *Deloix regia*. The phytochemical compounds in the plant extracts such as and amino acid and flavonol were responsible for the bioreduction of Ag^+ ions to silver nanoparticles Ag^0, as indicated by FT-IR and UV vis. spectra. The size and morphology of silver nanoparticles were indicated using the TEM study to confirm the shape and size of the silver nanocrystals. Moreover, parameters such as dose, particle size, initial concentration, contact time and temperature effect on the biosorption process were studied. Furthermore, the mechanism of adsorption process was suggested to be ion-exchange mechanism. The synthesized nanoparticle (DREAgNPs) is eco- friendly, non-expensive and easily available adsorbent for adsorbing the Cu^{2+} ions from an aqueous solution.

COMPETING INTERESTS

Authors have declared that no competing interests exist.

REFERENCES

1. (a) Ali DM, Thajuddin N, Jeganathan K, Gunasekaran M, Plant extract mediated synthesis of silver and gold nanoparticles and its antibacterial activity against clinically isolated pathogens. Colloids Surf. B Biointerfaces. 2011;85:360 – 365. (b) El-Remaily MA, Abu-Dief AM, Rafat M. El-Khatib. A robust synthesis and characterization of superparamagnetic CoFe2O4 nanoparticles as an efficient and reusable catalyst For green synthesis of some heterocyclic rings, Appl. Organomet. Chem. 2016;30:1022–1029. (c) Ahmed M.

Abu-Dief, Nassar I.F, Elsayed WH. Magnetic NiFe2O4 nanoparticles: Efficient, Heterogeneous and reusable catalyst for synthesis of acetylferrocene chalcones and their anti-tumour activity, Appl. Organomet. Chem. 2016;30:917–923. (d) A.M.Abu-Dief, S. M. Abdel-Fatah, Development and functionalization of magnetic Nanoparticles as powerful and green catalysts for organic synthesis. Beni-SuefUniv. J. Basic Appl. Sci. 2018;7:55–67. (e) Abu-Dief AM, Mohamed WS, α-Bi2O3 nanorods: Synthesis, characterization and UV-photocatalytic activity, Mater. Res. Express. 2017;4:035039.

2. Ahmad N, Sharma S, Alam Md K, Singh VN, Shamsi S F, Mehta BR, Fatma A. Rapid synthesis of silver nanoparticles using dried medicinal plant of basil. Colloids Surf. B Biointerfaces. 2010:81:81–86.
3. Mollick MdMR, Bhowmick B, Maity D, Mondal D, Roy I, Sarkar J, Rana D, Acharya K, Chattopadhyay S., Chattopadhyay D. Green synthesis of silver nanoparticles-based nano fluids and investigation of their antimicrobial activities. Microfluid. Nanofluid. 2014;16: 541–551.
4. (a)Singh A, Jain D, Upadhyay MK, Khandelwal, N, Verma HN. Green synthesis of silver nanoparticles using Argemonemexicana leaf extract and evaluation of their antimicrobial activities. Dig. J. Nanomater. Biostruct. 2010;5:483–489; (b) Mahmoud Abd El Aleem Ali Ali El□Remaily, Ahmed M Abu□Dief, O Elha, Green synthesis of TiO2 nanoparticles as an efficient heterogeneous catalyst with high reusability for synthesis of 1, 2□dihydroquinoline derivatives, Applied Organometallic Chemistry. 2019;33(8): e5005.
5. Retchkiman-Schabes, PS, Canizal G, Becerra-Herrera, R, Zorril-la C, Liu HB, Ascencio JA. Biosynthesis and characterization of Ti/Ni bimetallic nanoparticles. Opt. Mater. 2006;29:95 – 99.
6. Gu H, Ho PL, Tong E, Wang L, Xu B, Presenting vancomycin on nanoparticles to enhance antimicrobial activities. Nano Lett. 2003;3:1261–1263.
7. Ahmad Z, Pandey R., Sharma S, Khuller GK. Alginate nanoparticles as antituberculosis drug carriers: formulation development, pharmacokinetics and therapeutic potential. Indian J. Chest Dis. Allied Sci. 2005;48:171–176.
8. Bankura K P, Maity D, Mollick M.M.R., Mondal D, Bhowmick B, Bain MK, Chakraborty A, Sarkar J, Acharya K, Chattopadhyay D. Synthesis, characterization and antimicrobial activity of dextran stabilized silver nanoparticles in aqueous medium. Carbohydr. Polym. 2012;89:1159–1165.
9. Farooqui MA, Chauhan PS, Krishnamoorthy P, Shaik J. Extraction of silver nano-particles from the leaf extracts of Clerodendruminearme. Dig. J. Nanomater. Biostruct. 2010;5:43–49.
10. Cho K, Park J, Osaka T, Park S. The study of antimicrobial activity and preservative effects of nanosilver ingredient. Electrochim. Acta. 2005;51:956–960.
11. Elumalai EK, Prasad TNVKV, Hemachandran J, Therasa SV, Thirumalai T, David E. Extracellular synthesis of silver nanoparticles using leaves of Euphorbia hirta and their antibacterial activities. J. Pharm. Sci. Res. 2010;2:549–554.
12. Safaepour M, Shahverdi AR, Shahverdi HR, Khorramizadeh M.R, Gohari AR. Green synthesis of small silver nanoparticles using geraniol and its cytotoxicity against Fibrosarcoma-Wehi 164, Avicenna. J. Med. Biotechnol. 2009;1: 111–115.
13. Awwad A. M, Salem N.M. Green synthesis of silver nanoparticles by mulberry leaves extract. Nanosci. Nanotechnol. 2012;2:125 – 128.
14. Chandran S. P, Chaudhary M, Pasricha R. Synthesis of gold nanotriangles and silver nanoparticles using Aloe vera plant extract. Biotechnol. Progr. 2006;22:577–583.
15. Sathishkumar M, Sneha K, Won SW. Cinnamon zeylanicum bark extract and powder mediated green synthesis of nano-crystalline silver particles and its bactericidal activity. Colloids Surf. B Biointerfaces. 2009;73:332–338.
16. Jain D, Kumar daima H, Kachhwaha S, Kothari SL. Synthesis of plant-mediated silver nanoparticles using papaya fruit extract and evaluation of their anti microbial activities, Dig. J. Nanomater. Biostruct. 2009;4:557–563.
17. Ahmad N, Sharma S, Singh VN, Shamsi SF, Fatma A, Mehta B.R. Biosynthesis of silver nanoparticles from Desmodiumtriflorum: A novel approach towards weed utilization, Biotechnol. Res. Int. 2011;1:454090.
18. Zaheer Z, Rafiuddin, Bio-conjugated silver nanoparticles: From Ocimum sanctum and role of acetyltrimethyl ammonium bromide, Colloids Surf. B Biointerfaces. 2013; 108:90–94.
19. Ali, E N, Alfarra, S. R., Yusoff, M. M, Rahman M L. Environmentally Friendly Adsorbent from Moringa Oleifera Leaves for Water Treatment. Int. J. Environ. Sci. Dev. 2015: 6: 165 – 169.

20. Abdel-Rahman L H, Abu-Dief A M, Abd-El Sayed M A, and Zikry M M., Nano Sized Moringa oleifera an Effective Strategy for Pb (II) ions Removal from Aqueous Solution, J. Chem. Mater. Res. 2016a:8 (4): 8-22.
21. Abdel-Rahman L H, Abu-Dief Ahmed M, Abd-El Sayed M A and Zikry M M, Disposal of Heavy Transition Cd2+ Ions from Aqueous Solution Utilizing Nanosized Flamboyant Pod (Delonix regia). J. Trans. Metal Complexes, :2018: 1
22. Darroudi M, Ahmad M, Abdullah A, Ibrahim N, Shameli K, Int. J. Mol. Sci. 2010;11 :3898.
23. Fafal T, Taştan P.B, Tüzün S, Ozyazici M, BijenKivca k. Synthesis, characterization and studies on antioxidant activity of silver nanoparticles using AsphodelusaestivusBrot. aerial part extract, South African Journal of Botany. 2017;112:346 –353.
24. Xie J, Lee JY, Wang DIC, Ting YP. Silver nanoplates: from biological to biomimetic synthesis, ACS Nano. 1. 2007;429 – 439.
25. Saifuddin N, Wong CW, NurYasumira AA. Rapid biosynthesis of silver nanoparticles using culture supernatant of bacteria with microwave irradiation, E-J. Chem. 2009;6:61–70.
26. Rao B, Tang RC. Green synthesis of silver nanoparticles with antibacterial activities using aqueous Eriobotrya japonica leaf extract. Adv. Nat. Sci.: Nano sci. Nanotechnol. 2017;8:015014.
27. Pons MN, Bonte SL, Potier O. Spectral analysis and fingerprinting for biomedia characterisation. J. Biotechnol. 2007;113: 211- 230.
28. Boparai HK, Joseph M, O'Carroll DM. Kinetics and thermodynamics of cadmium ion removal by adsorption onto nano zero valent iron particles, J. Hazard. Mater. 2011;186:458–465.
29. N. Alaguchamy, M. Chandran, W j Pharma Pharm Scie. 2016;5(11).
30. Biswas T, Sen A, Roy R, Maji S, Maji HS. Pharmaceutical Analysis Isolation of Mangiferin from Flowering Buds of Mangiferaindica L and its Evaluation of in vitro Antibacterial Activity. 2015;4:49–56.
31. Elavazhagan T, Arunachalam KD. Memecylonedule leaf extract mediated green synthesis of silver and gold nanoparticles, Int. J. Nanomed. 2011;6: 1265–1278.
32. Alam MN, Roy N, Mandal D, Begum NA. Green chemistry for nano chemistry: exploring medicinal plants for the biogenic synthesis of metal NPs with fine-tuned properties. RSC Adv. 2013;311935–11956.
33. Coates J, Interpretation of Infrared Spectra, a Practical Approach, Encyclopedia of Analytical Chemistry, John Wiley & Sons, Ltd; 2006.
34. Swarnavalli G C J, Dinakaran S, Raman N, Jegadeesh R, Carol Pereira. Bio inspired synthesis of mono dispersed silver nanoparticles using Sapindusemarginatus pericarp extract – Study of antibacterial efficacy, Journal of Saudi Chemical Society. 2017;21:172-179.
35. Abu-Dief A M, Abdel-Rahma L H, Abd-El Sayed MA, Zikry M M, and Nafady A. Green Synthesis of AgNPs(0) Ultilizing Delonix Regia Extract as Anticancer and Antimicrobial Agents. Chemistry Select, 2020;5:13263-13268.
36. Bhatti H N, Nasir AW, Hanif MA, Efficacy of Daucuscarota L. waste biomass for the removal of chromium from aqueous solutions. Desalination. 2010;253:78-87.
37. Tavker N, Yadav VK, Yadav K K, Cabral-Pinto M M S, Alam J, Shukla, A K, Ali F AA, and Alhoshan M. Removal of Cadmium and Chromium by Mixture of Silver Nanoparticles and Nano-Fibrillated Cellulose Isolated from Waste Peels of Citrus Sinensis. Polymers. 2021;13:234.
38. (a)Abu-Gharib, EA, EL-Khatib, RM, Nassr, LAE, Abu-Dief AM. Kinetics of base hydrolysis of some chromen-2-one indicator dyes in different solvents at different temperatures. Journal of the Korean Chemical Society. 2011;55(3):346-353; (b) Abu-Gharib, EA, EL-Khatib, RM, Nassr, LAE, Abu-Dief AM. Kinetics, reactivity, initial-transition state analysis and thermodynamic parameters of base-catalyzed hydrolysis of coumalic acid in solvents with different polarities. Arabian Journal of Chemistry.2017;10:S988-S995; (c) Ahmed M. Abu-Dief, Rafat M El-khatib, Faizah S Aljohani, Seraj Omar Alzahrani, Asmaa Mahran, Mohamed E Khalifa, Nashwa M El-Metwaly, Synthesis and intensive characterization for novel Zn (II), Pd (II), Cr (III) and VO (II)-Schiff base complexes; DNA-interaction, DFT, drug-likeness and molecular docking studies, Journal of Molecular Structure 2021; 11242:130693
39. Abdel-Rahman LH, Al-Farhan BSF, Abu-Dief AM, Zikry MM. Removal of Toxic Pb(II) Ions from Aqueous Solution by Nano Sized Flamboyant Pod (Delonix regia). Arch Chem Res. 2016b;1:1.
40. Yavuz O, Altunkaynak Y, Gu¨zel F. Removal of copper, nickel, cobalt and manganese from aqueous solution by kaolinite. Water Res. 2003;37:948– 952.
41. Srivastava SK, Singh AK, Sharma A. Studies on the uptake of lead and zinc by lignin obtained from black liquoar: a paper industry

waste material. Environ. Technol. 1994:15:353-361.
42. Hasar, H. Adsorption of nickel (II) from aqueous solution onto activated carbon prepared from almond husk. J .Hazard .Mater. B. 2003;97:49-57.
43. (a)Hany M. Abd El-Lateef, Ahmed M. Abu-Dief, Bahaa El-Dien M. El-Gendy, Investigation of adsorption and inhibition effects of some novel anil compounds towards mild steel in H2SO4 solution: Electrochemical and theoretical quantum studies, Journal of Electroanalytical Chemistry 2015;758:135–147;(b) Hany M. Abd El-Lateef, Ahmed M. Abu-Dief, Mounir A.A. Mohamed, Corrosion inhibition of carbon steel pipelines by some novel Schiff base compounds during acidizing treatment of oil wells studied by electrochemical and quantum chemical methods, Journal of Molecular Structure. 2017;1130:522-542.
44. Namasivayam, C., Yamuna RT. Adsorption of chromium in tanned leather gloves and relapse of chromium allergy from tanned leather samples. Analyst. 1995:123:935-937.
45. Weber, Jr WJ. Physico-Chemical Processes for Water Quality Control. John Wiley and Sons Inc, New York, NY; 1972.
46. Stephen IB.; Chien JT.; Ho, GH.; Yang J.; Chen BH. Equilibrium and Kinetics Studies on Sorption of Basic Dyes by a Natural Polymer (γ – Glutamic Acid). Biochem. Eng . J. 2006:31:204-215,
47. Juang, LC; Wang, CC; Lee, CK. Biosorption of Basic Dye onto MCM-41. Chemosphere. 2006:64:1920-1928.
48. Jain CK, Singhal DC, Sharma MK. Adsorption of zink on bed sediment of River London: adsorption models and kinetics. J. Hazard. Mater. B. 2004;114: 231.
49. Ozcan, AS and Ozcan A. J. Colloid Interface Sci. 2004;276:39.
50. Dursun AY. A comparative study on determination of the equilibrium, kineticand thermodynamic parameters of biosorption of copper and lead ions ontopretreated Aspergillusniger, Biochem. Eng. J. 2006; 28:187–195.
51. Meena AK, Mishra GK, Rai PK, Rajagopal, C.; Nagar, PN. Removal of heavy meal ions from aqueous solutions using carbon aeogel as an adsorbent. J. Hazard. Mater. 2005;122:161-170.
52. Niu Z, Li Y. Removal and utilization of capping agents in nanocatalysis. Chem Mater. 2014;26:72–83.
53. Gulati S, Sachdeva M, Bhasin KK. Capping agents in nanoparticle synthesis: csurfactant and solvent system. AIP Conf Proc. 2018;1953:030214.
54. Potara M, Focsan M, Craciun A-M, Botiz I, Astilean S. 15-Polymer-coated plasmonic nanoparticles for environmental remediation: Synthesis, functionalization, and properties. In: Hussain CM, Mishra AK, editors. New polymer nanocomposites for environmental remediation; 2018;361– 87.
55. Aashima, Mehta SK. Chapter 18 - Impact of functionalized nanomaterials towards the environmental remediation: challenges and future needs. In: Mustansar Hussain C, editor. Handbook of functionalized nanomaterials for industrial applications. 2020:505–24.
56. Javed R, Zia M, Naz S, Aisida S O, Ain N, Qiang A. Role of capping agents in the application of nanoparticles in biomedicine and environmental remediation: Recent trends and future prospect. J Nanobiotechnol. 2020;18:172-187.

Peer-review history:
The peer review history for this paper can be accessed here:
https://www.sdiarticle4.com/review-history/70878